Measuring forces and stresses in situ in living tissues

by: "Forces in tissue" workshop participants[1]

Abstract

In living tissues, genetics and mechanics interact, especially during morphogenesis. Two main classes of mechanical measurements are already established: live imaging helps quantifying tissue deformation, cell-level dynamics, and protein distributions; cell or tissue rheology yields access to material properties such as elastic stiffness and viscosity. The third one, measuring forces and stresses in situ at scales ranging from molecule to cell and to tissue, involves different challenges. We review several emerging techniques, their fields of applications, their advantages and limitations, their validations. We argue that they will strongly impact our understanding of developmental biology in the near future.

I - Introduction

During animal development, tissues undergo extensive morphogenesis based on coordinated changes of cell shape and position over time. Such developmental processes, like other biological phenomena, are under the control of genetics, chemistry, and physics. Genetic information is translated into biochemical signaling, which regulates body axis determination, tissue patterning, sequence and timing of cell divisions and differentiations. Mechanics provides another layer of regulations of development, as evolutionally conserved as is biochemical signaling (Savin et al., 2011; Brunet et al., 2013), and also contributing to plant development (Sampathkumar et al., 2014). Mechanics acts for instance through size, position or shape changes inside cells, at the cell level or within a group of cells: these changes are required for genetics to translate into actual cell organisation and tissue shape.

Genetics and mechanics mutually feedback on each other. Disentangling their respective contributions benefits from quantitative characterisation of the physical mechanisms at play. Two main classes of mechanical measurements are already established (Fung, 1993; Oates et al., 2009; Labouesse, 2011): live-imaging, and cell or tissue rheology. The third class is measurements of force and stress (Fig. 1), which has been up to now mainly established *in vitro* (Paluch, 2015). Forces with which cells pull and push on their neighbours or environment during development deform tissue to its final size and proportion, orient cell polarity, control transcription program of cell differentiation (Lecuit et al., 2011; Mammoto et al., 2012; Heisenberg and Bellaïche, 2013; Sampathkumar et al., 2014). Understanding force generation and sensation, feedbacks and integration of genetics and mechanics would therefore lead us to a comprehensive picture of development, linking the scales of intra-cell components, cell, group of cells, and tissue. It would also improve our understanding and diagnosis of muscle defects and other force-related diseases.

Live movies (or "kinematics") yield details on cell shape, size, position, neighbours and number, as well as on tissue shape and size, and changes thereof. Material properties (or "rheology") include viscosity, stiffness and yielding, which respectively characterise a liquid, an elastic solid and a plastic solid. Actions (or "dynamics") such as forces and stresses arise mainly from the distributions and regulation of molecular motors. Understanding and modeling the role of mechanics in morphogenesis should incorporate: different scales from cell level (or from molecule level) to tissue level; both solid-like and liquid-like mechanical behaviours; cell mechanical activity due to molecular motors; coupling biochemical and mechanical regulations. In simple materials with known liquid or solid properties, movies would suffice to predict actions, and vice versa. Conversely, in living tissues, forces cannot simply be deduced from live imaging and cell rheology: movies and actions should be incorporated in models to infer the complex material properties. Direct force and stress measurement in a living organism is a prerequisite. Ideally, it should yield real time, non-destructive space-time maps of absolute values with good signal-to-noise ratio and independent validations. Addressing this challenge is a recent and blowing field of research.

We review here corresponding measurement methods (Fig. 2). We explain which quantity they measure, specify their accessible range, and compare their advantages (Table 1). We explicit their underlying hypotheses, and mention when they are applicable to plants too. We hope to help newcomers in the field to select techniques appropriate to their studies, encourage the formation of a community with common cross-validation methods, and improve the integration of mechanics data into models to deepen our understanding of physical principles of development.

[1] Address correspondance to: tissue.stress@univ-paris-diderot.fr

II - Methods

- Tweezers: magnetic, optical

Optical or magnetic "tweezers" refer to set-ups that apply forces to transparent or magnetic objects through gradients of light intensity or magnetic field, respectively (Fig. 2A, B). The methods are non-invasive, as they allow micromanipulation without direct contact.

The working principle of magnetic tweezers is that a magnetic particle in a magnetic gradient will be subject to a force directed toward the source of the field (Fig. 2A top). The force depends on the magnetic properties and geometry of the particle used as well as the intensity profile of the external field. Magnetic fields are produced either by permanent magnets or electromagnets, which are mounted on a microscope stage and can come in different designs depending on the specific application pursued (Tanase et al., 2007).

The working principle of optical tweezers is that a transparent particle (showing a higher refraction index than the surrounding) in a focused beam is subject to a gradient force pulling it toward the high intensity region (focus) of the beam, while a scattering force pushes it away from the focus in the direction of incident light (Fig. 2B top). An effective optical trap occurs when the gradient forces dominate over the scattering forces. The optical force is a function of the geometry and refractive properties of the particle as well as the intensity profile of the optical field. Optical tweezers can be combined to most microscope setups as the infrared laser used to produce laser trap is focused by the same objective lens as the one used for image collection.

Both methods usually rely on the introduction of particles such as beads of micrometer size; however, as some organelles show refraction index mismatch with the surrounding, optical tweezers can eventually be applied directly without the use of a particle. In both methods, the displacement of the tweezed object indicates the nature and the magnitude of the mechanical resistance, which opposed to the applied force; the resistance can be elastic, viscous or a combination of both properties (viscoelastic material). Tweezers experiments can yield access to both force (or tension) and viscoelastic measurements. The forces are typically on the order of pico- to nanoNewtons with magnetic tweezers and on the order of picoNewtons with optical tweezers.

Despite their potential advantages with regard to contact techniques, tweezers experiments have up to now mostly been used for cell rheology. To provide quantitative force measurements, they require *in situ* calibration, which might turn out to be delicate in living tissues. To date magnetic tweezers have been used in *Drosophila* to produce tissue scale deformation thanks to the injection of large volumes of ferrofluid in the early embryo (Desprat et al., 2008). Recently optical tweezers have shown to be applicable either using beads or by direct trapping in the early *Drosophila* embryo to measure forces at cell junctions and delineate the propagation of deformation in the plane of the tissue (Bambardekar et al., 2015; Fig. 2B bottom).

- FRET

Förster resonance energy transfer (FRET) is an energy transfer between transition dipoles of two fluorophores (Fig. 2C), namely donor and acceptor (Miyawaki, 2011). Its efficiency E sharply depends on the distance R between fluorophores, as a power 6: $E = R_0^6/R^6+R_0^6$, where R_0 is the distance where FRET efficiency is 50 % (Fig. 2C bottom left). Measuring its efficiency is thus highly sensitive to variations in R, hence its nickname "spectroscopic ruler".

Now, if a spring of known stiffness is inserted between donor and acceptor fluorophores, the change is spring length enables to infer the tension in the spring. A tension sensor such as a polypeptidic elastic spring, and a series of control probes are genetically encoded and inserted into a protein of interest, by using standard molecular biology techniques, to report the tension in that protein (Meng et al., 2008; Grashoff et al., 2010; Fig. 2C top).

FRET efficiency or index is measured by changes in fluorescence lifetime, spectral changes, or ratios of intensities. The measurement is scalar and its dynamic range depends on the elasticity of spring; e.g. in Grashoff et al., (2010) the probe is most sensitive to 1 to several pN forces. This is an ensemble measurement, though single molecule FRET could be done in principle. The method has been successfully applied to adhesion and cytoskeleton-related proteins in *in vitro* and *in vivo* model systems (Grashoff et al., 2010; Borghi et al., 2012; Krieg et al., 2014; Cai et al., 2014). The major advantage of the method is that it could be applicable to any protein of interest as long as the tagged protein retains the function and nature of the native protein. In addition, it is compatible with imaging of other proteins and/or structures and with mechanical manipulation.

The high sensitivity of the FRET efficiency vs force relation makes its calibration (Fig. 2C bottom right) crucial, especially if absolute values of force measurements are expected. Some already calibrated standard constructs are

available. Else, after probe synthesis, calibration should be performed *in vitro*, for instance by single molecule measurement. The method assumes that inserting tension sensor module into a host protein does not change the efficiency-force relation, that other factors (e.g., time-average of orientation alignment of donors and acceptors) remain constant during a measurement and in different probes, and that the calibration *in vitro* remains valid *in vivo*.

More generally, fluorescent materials exhibit a variety of properties that could be dependent on mechanics (Gomez-Martinez et al., 2013; Watanabe et al., 2013).This opens up an opportunity to design and develop new force probes in the near future.

- Birefringence : **internal, external**

When an otherwise isotropic material is subject to a stress, its electronic structure differs in the directions of larger and smaller stresses. Such material, said to be "birefringent" (Fig. 2D), becomes optically anisotropic: its refractive indices in both directions n_1, n_2 differ by a term proportional (up to the so-called "photo-elastic constant" c which characterises the material) to the stress differences along both axes. By placing it between two crossed polarisers, each oriented at 45° from the main stress directions (Fig. 2D, top), the transmitted light intensity varies as a squared cosine of the index difference n_1-n_2 times the material thickness d.

The material thus acts as an indirect stress probe (Fig. 2D, bottom), which sensitivity is determined by both c and d. The object studied should be flat (or the profile of d is known), transparent and homogeneous. Measurements are non-destructive, and simple if stress is the only cause of anisotropy. The signal is integrated along the z-axis, so the information is mapped in the xy plane, and its space-time resolution is that of the camera. A crude version can be implemented on any microscope or with any camera for a few Euros. The resolution can be improved by: using a liquid crystal retarder (for a few kEuro), optimizing image processing (Shribak and Oldenbourg, 2003), or using several polarizer and analyzer orientations which in addition determines the stress directions.

The relative precision can reach 10% while absolute calibrations require the determination of c, which is delicate *in vivo*. Within a tissue, c can be measured in an explant if birefringence measurements are combined with a micro-manipulation setup to apply a stress. In *Drosophila* wing discs (Nienhaus et al., 2009), but also in other tissues (plants, trachea) the photoelastic constants are of the order of 10^{-10} Pa^{-1} and stresses of 10 kPa are detectable (Schluck and Aegerter, 2010). Soft embryonic tissue requires forces in the range of sub-µN, adult or larval tissues are in the 100 µN range, plant tissues are in the 1-10 mN range; in a plant meristem, a typical range of measured stress is 2 to 500 kPa. Forces exerted by cells on a solid substrate down to 1 pN per square microns have been measured (Curtis et al., 2007).

Alternatively, the birefringence of an external sensor placed in contact with the tissue yields a pattern of optical fringes related to the stress field in the sensor (Fig. 2E, top). This yields semi-quantitatively the force exerted by the tissue on the sensor (to make it quantitative requires to assume that the photoelastic material is truly linear, and to solve inverse problems which are sometimes difficult). It is biocompatible, non-destructive and suitable for living systems above a millimeter that move and/or grow. This was used to quantify radial force down to one Newton during root growth in response to constraints (Fig. 2E, bottom) (Kolb et al., 2012). Validation is direct if the photoelastic material is well calibrated: either commercial (a few hundred euros for a sheet in which several sensors can be cut), or preliminary calibrated plexiglass or agar gels.

- Liquid drops

Liquid drops can be used as versatile stress sensors (Campàs et al., 2014) (Fig. 2F). The shape of a drop contributes to its energy as the surface tension multiplied by the surface area. At rest, the drop minimises its surface, and is spherical. When a drop is introduced between cells in a tissue, it is deformed by local stresses. Fluorescence microscopy yields the drop contour. Provided the drop surface tension is separately measured, image analysis directly infers how anisotropic is the stress locally exerted on the drop by the neighboring cells or the extracellular matrix (equation in Fig. 2F).

Producing the drops requires fine chemistry, which costs more in term of work than of reagents (typically hundreds of euros). Drops should be fluorescent, cell-sized; made of bio-compatible oil, but not internalized by neighbouring cells; coated with surface integrin or cadherin receptor ligands, in order to be pulled (and not only pushed). The equipment includes a fluorescent microscope, preferably three-dimensional; a tensiometer; and a micro-injector. Injecting at the right place, and making sure there is an effective link with the cell adhesion molecules of neighbouring cells, is one of the most delicate parts of the manipulation.

The drop contour is measured at video frequency, and analysed a posteriori. The experiment can last for days without affecting for instance an embryo, where muscle forces are probed during development. The drop size is at maximum of order of 600 micrometers, to be really spherical at rest. It is at least 5 micrometers, to avoid being internalised by cells,

but the stresses themselves can be measured at a much smaller size, typically a few pixels. Measured forces and stresses are in the range 4 to 30 mN/m and 0.3 to 60 kPa, respectively.

Drop contour curvatures can be measured up to 5% accuracy, so that the limiting factor is the precision of surface tension measurement, around 20%. This relies on the hypothesis that the surface tension remains constant and uniform when the drop is introduced between cells. Such hypothesis is reasonable if the drop surface has been beforehand saturated in proteins, eg BSA, but should be validated independently.

Although cells may react on their neighbours stiffness, tests yield the same measurement of stress for cells in aggregates or in tissues, and for drops with small or large surface tension, lending confidence to the method's validity and reproducibility. An additional check is that when cells die, drops immediately recover their spherical shape.

This method has already been used to prove that anisotropic stresses generated by mammary epithelial cells are dependent on myosin II activity (Campàs et al., 2014). They apply to both mesenchymes and epithelia, where the drop is only partially embedded and displays a free surface (so that it becomes possible to measure the pressure too). Perspectives include: more stable drops; applications to fish and chicken embryonic tissues; also possibly flatworm, fly; adult organs including tumors.

A possible variant would consist in replacing the liquid drop with a soft spherical elastic bead. If deformations remain small, fitting an ellipsoid to the bead contour would yield the main directions of stress applied by cells on the bead. The change in bead volume measures the pressure or traction in the surrounding tissue. The beads could be made of polymers in a microfluidic setup; their rigidity (Young modulus) should be adjusted, typically around 1 kPa, and carefully calibrated. Alternatively, embedding a Xenopus embryo in an external soft agarose gel has already enabled to estimate the forces it develops during convergent extension (Zhou et al., 2015).

- Micro-manipulation: indentation, aspiration

Micro-manipulation (Fig. 2G, H) can be performed by applying an external force using tools such as microplates, indenters or pipettes (Davidson and Keller, 2007). It applies to single cells or to tissues, which are directly accessible, without rigid external layer. It normally determines the material rheology; for instance, the elastic modulus is calculated from the initial deformation, and the viscosity from the long term constant flow rate (Fig. 2H right). Micro-manipulation yields measurements of internal forces and stresses when they directly influence the material rheology. This is notably the case for turgor pressure in plants, which contribution to the cell wall resistance can be explicitly separated from the cell wall visco-elastic properties (Forouzesh et al., 2013; Beauzamy et al., 2014).

Between parallel microplates, one of which being a force transducer, uniaxial compression is applied on a large surface area of the sample causing the sample undergo strain (Foty et al., 1994; Fig. 2G top left). Indenters are rods or shaped cantilever tips (in atomic force microscopes), which push on the sample across a small contact area (Lomakina et al., 2004; Fig. 2G top right). In micropipettes, an aspiration causes the deformation of the sample across the aperture of the pipette. It requires an (inverted) microscope, a micromanipulator and a pressure device.

Pipette aspiration has been used to measure cell wall tension of single cells (Krieg et al., 2008) and study their actomyosin cortex (Paluch and Heisenberg, 2009). The equilibrium shape of the cell into a pipette results from the balance of its wall tension produced by its contractile cortex (Evans and Yeung, 1989) and the pressure aspiration. The aspiration pressure is tuned at the critical value at which the cell deforms in the pipette to form a hemisphere with a radius equal to the radius of the pipette (Fig. 2H left). The cell wall tension can be then simply determined from the pressure in the micropipette and the radii of the cell inside and outside the micropipette (Young-Laplace law): typical values range between tens of µN/m and tens of mN/m.

Similarly, microplates or pipettes have been used for tissue explants and cell aggregates. Surface tension measurements require a few minutes and provide absolute values with precision of a few percents: the biological variability dominates the experimental uncertainty. Surface tensions between tens of µN/m and tens of mN/m have been measured on cell aggregates (Guevorkian et al., 2010, Marmottant et al., 2009) or zebrafish embryos (Maître et al., 2012). With applied forces ranging between 0.1-10 µN, elastic moduli of few hundreds of Pa and viscosities of hundreds of kPa.s have been measured on cell aggregates. In the near future one expects to see results on single cells in live embryos, eg in mouse.

- Laser ablation: sub-cellular scale, **tissue scale**

Laser ablation experiments consist in severing biological structures taking part in the force transmission across the tissue (cytoskeletal filaments, cell junctions) in order to provoke a sudden force imbalance (Fig. 2I, J). The dynamics of

relaxation after severing is governed by the remaining stresses and the friction forces.

In subcellular ablation, a tightly focused laser is targeted at cell-cell contacts to disrupt the biological structures which support tensile forces (actomyosin network). This results in a force imbalance, which drives changes in cellular geometries (cell vertex displacement for instance). Assuming the tissue was in equilibrium before ablation, the speed of relaxation just after ablation is a local measure of cell junction tension to dissipation ratio (Fig. 2I). It can be used as a proxy for tension measurement, keeping in mind that it yields relative rather than absolute values of tension, and relies on the assumption that the viscosity changes much less than the tension.

As it is a non-contact method, laser ablation can be applied to a large variety of tissues in different organisms such as *Drosophila* (Farhadifar et al., 2007; Kiehart et al., 2000; Rauzi et al., 2008) or C. elegans (Mayer et al., 2010). Relaxation measurements after ablation require a few minutes and can be repeated few times in the same sample (at different positions in the embryo). The animal usually heals and apparently develops normally.

The method can be easily combined with different types of microscopes using simple optical elements. Molecular bond rupture and laser-induced plasma formation (by generation of free electrons) are the main processes underlying laser ablation. Their production depends on different parameters such as laser wavelength, power density, temporal compaction of photons (pulse duration) and pulse repetition rate (Vogel and Venugopalan, 2003). In practice two types of laser are used in living tissues. Ultra-violet nanosecond pulsed laser is cheaper, and it is easier to set a suitable light intensity. Near-infrared femtosecond pulsed laser (NIR-fs) offers the advantage to produce very few collateral damages and has been shown to preserve membrane integrity, while allowing disruption of single adherens junctions (Rauzi et al., 2008).

Enlarging the scale, a laser can simultaneously ablate several cells (Hutson et al., 2003; Behrndt et al., 2012). The initial velocity measures the stress-to-viscosity ratio within the tissue, in the direction perpendicular to the ablation line. Alternatively, severing a large circle (Bonnet et al., 2012) reveals the main directions of stress and its anisotropy (Fig. 2J). In addition, having isolated a piece of tissue reveals its final relaxed stated, yielding the strain along different orientations with percent accuracy. With additional hypotheses and a model, information can be obtained about the ratio of external friction to internal tissue viscosity.

The ablation time and the time between successive images should be less than a second to remain much shorter than the relaxation time. The maximal ablation scale is determined by the tissue curvature, since all cells junctions to be severed should be simultaneously in focus. Proper axial and lateral alignment is required for efficient and well-controlled ablation experiments, and becomes crucial for the large scale circular version.

At even larger scale (millimeters), the same principle applies when cutting with a scalpel a tissue under tension (Fung 1993). In flat tissues such as a floating biofilm, absolute values in the milliNewtons are measured up to percent precision in an inexpensive set-up using a standard force sensor (Trejo et al. 2013).

- Force inference: static, dynamic

In epithelial tissues where cell shapes are determined by cell junction tensions and cell pressures, i.e. assuming mechanical equilibrium, information on force balance can be inferred from image observation (Fig. 2K). For instance, if three cell junctions which have the same tension end at a common meeting point, their respective angles should be equal by symmetry, and thus be 120° each. Reciprocally, any observed deviation from 120° yields determinations of their ratios. The connectivity of the junction network adds redundancy in the system of equations, since the same cell junction tension plays a role at both ends of the junction.

Mathematically speaking, there is a set of linear equations, which involve all cell junction tensions, and cell pressure differences across junctions. The coefficients of these equations are determined from observation of vertex positions. The number of unknown can be larger or smaller than the number of equations, resulting in under- or over-determination, respectively. According to the mechanical and morphological properties of the system of interest, one of the following variants could be chosen.

Treating cell junctions as straight and neglecting pressure differences results in overdetermination (Chiou et al., 2012). Treating more general cases which are underdetermined, for instance when taking into account the pressure differences (assuming small cell curvatures), is possible using Bayesian force inference: it treats the ill-conditioned problem and simultaneously estimates tensions and pressures by using Bayesian statistics (Ishihara and Sugimura, 2012; Ishihara et al., 2013; Sugimura and Ishihara, 2013). Adding visual observation of cell junction curvature brings back to overdetermination, by including the Young-Laplace law that relates the cell junction curvature to tension and pressure (Brodland et al., 2014).

These variants of the inverse problem infer tension to only one unknown constant, the tension scale factor, whether for a few cells or for a few thousands. In the latter case, detection of contours of thousands of cells and precise measurement of the cell contact surface curvature requires a sophisticated image processing algorithm. When pressures are determined, there is an additional unknown constant, the average cell pressure. By integrating tensions and pressures, tissue stress can be calculated at all places, again up to these two constants. These constants are not visible on the image: if they are necessary, they have to be determined by another method.

The advantages of force inference are as follows. First, it offers both single cell resolution and a global stress map, which allows to compare the inferred forces directly with the activity of the molecules and with the cell-level dynamics, as well as with their effect on tissue scale. Second, it is non-destructive, so that the dynamics of forces or stresses can be analysed along a live imaging movie in two or three dimensions. Third, the method is free from any assumption regarding the origin of tension and pressures (unlike analytical or numerical models which assume contributions of cell-cell adhesion or cell wall cortex contractility). Fourth, force inference lends it well to various validations, for instance against myosin distribution; tests on a controlled pattern prepared using numerical simulations have shown its accuracy and robustness to added noise. It is also suitable to perform cross-validations against other measurement methods (see below).

For more quickly evolving tissues, a dynamic version of force-inference called "video force microscopy" assumes the type of dissipation and uses temporal cell shape changes to infer forces. The original version solved an over-determined problem with a special three-dimensional geometry of cells (Brodland et al., 2010). A revised version is applicable to a general epithelial geometry (Brodland et al., 2014).

III - Discussion

- Comparison

Measuring forces is one contribution to our understanding of the link between the scales of intra-cell components, cell, group of cells, and tissue. It is thus relevant to probe forces at different scales, and integrate them into tissue-scale description in terms of stresses. This is possible by changing technique; or by changing scale within one given technique, e.g. pipettes or ablations range from a single cell junction to a large group of cells. Measurements obtained using a small scale probe can be gathered and presented at a much larger scale: FRET, force inference and birefringence are measured at the scale of molecule, cell junction and group of cells, respectively, but each can yield a tissue-scale map of stress measurements (which, incidentally, can be checked by measuring their divergence, which should be zero in absence of any external force).

Together, the above techniques probe a wide range of force scales. Again, some of these techniques can in turn be tuned to adapt to the object to probe: drops of different surface tensions, traps (optical or magnetic) or cantilevers of different stiffnesses. The time scales too vary widely but this is less important, since most measurements are actually recorded at the image acquisition rate which is typically a fraction of second, while the morphogenetic events have much longer characteristic times from hundreds to thousands of seconds; exceptions such as pipettes, which require hundreds of seconds, are suitable for slightly slower morphogenetic events.

Their results are complementary: drops, tweezers, pipettes, *in vitro* FRET, indentation and external birefringence yield absolute values, while internal birefringence, *in vivo* FRET, ablation or inference yield relative values up to an unknown prefactor. Methods such as birefringence apply mainly to thin tissues; FRET, ablation, indentation, pipettes or tweezers apply to tissue outer surfaces; force inference and drops apply to both two and three dimensions.

- Cross-validation

Repeating the same measurement with different techniques cross-validates them and yields more reliable results, which are less sensitive to choices and hypotheses, and help a consistent picture emerge. However, up to now, it is difficult to conceive a single system where all above methods could be used, due to their different requirements. Internal birefringence and optical tweezers require tissue transparency. Pipette and indentation act on cells accessible to direct mechanical contact. Drops and beads require injection. Force inference requires images where cell contour can be identified. *In vivo* FRET, force inference and ablations rely on hypotheses, which, although not yet directly proven, progressively gather consensus.

Pairwise comparisons of techniques on adequate systems are thus more promising. *In vitro* systems, in which most techniques can be precisely calibrated (e.g., a cultured cell monolayer probed using traction force microscopy or stretching devices), are useful for this purpose. Two different techniques can be cross-validated by comparing their

results on a same *in vitro* system such as cultured cell monolayer, cell aggregate, or even foams. Whenever simultaneous measurements are possible, for instance using drops coated with FRET sensors, they would yield a direct comparison.

In vivo, Bayesian force inference has been tested against cell junction ablation in *Drosophila*. In pupal epithelia, Bayesian force inference has been successfully compared to large-scale ablation anisotropy measurements (Ishihara et al., 2013) and photo-elasticity patterns (Ishihara and Sugimura, 2012). Force inference could itself become an absolute method if its unknown constants are determined independently, e.g. by optical tweezers. If validated by absolute measurement methods force inference could in turn serve as a common benchmark to validate other relative measurement methods. In the future, establishing more *in vivo* systems enabling for cross-validations will speed up the development of *in vivo* force/stress measurement methods.

- Combinations

Most of the methods we reviewed here are now ready to be applied to interrogate quantitatively the mechanics of cells and tissues in different organisms. It will be important to combine and apply them in a more integrated way. For instance the combination of molecular force probes (FRET sensors) with mechanical manipulation (e.g. optical tweezers) might reveal the connections between mechanical stress and the molecular basis of force transmission at cell-cell contacts. Moreover local force measurements (e.g. with ~~oil~~ drops) could feed more global approaches based on image analysis such as force inference.

Force and stress measurements will be crucial to understand how the tissue mechanical properties are related one to another, from the subcellular scale to the scale of whole organisms and from millisecond to hour timescales. It is likely that they will help us understand emergent properties of tissues, such as the fluid-like nature of tissues at the developmental timescales (hours) as a property arising from the relatively fast dynamics of cytoskeletal and adhesive structures, which generate and transmit forces. We also expect that combination of mechanical measurements with the fast-growing opto-genetic tools will unveil important connections between mechanics and biochemical signalling.

- Links with modeling

Models, whether based on analytical equations or numerical simulations, assist force and stress measurements in several respects (see Brodland, 2004; Anderson et al., 2007; Oates et al., 2009 for details of models used in tissue mechanics). They help to propose and design new force measurement techniques and experiments (Bonnet et al., 2012; Campàs et al. 2014; Bambardekar et al., 2015). They extract measurements of relevant parameters: either directly, or through fits of models to data (Hutson et al., 2003; Farhadifar et al., 2007; Ishihara and Sugimura, 2012; Brodland et al., 2010, 2014). They provide benchmark data, in controlled conditions, to validate an experimental measurement, and test its sensitivity to a parameter or to errors (Landsberg et al., 2009; Ishihara et al., 2013; Brodland et al., 2014; Bambardekar et al., 2015). They enable to extract more information from experimental results and refine their interpretation (Farhadifar et al., 2007; Krieg et al., 2008; Rauzi et al., 2008; Mayer et al., 2010; Bonnet et al., 2012; Sugimura and Ishihara, 2013; Forouzesh et al., 2013).

Biomechanical models are increasingly used in developmental biology (Keller, 2002). By determining which assumptions are sufficient to describe an experimental observation, they assist and complement genetic experiments. Models describe and reproduce phenotypes, predicting results and trying to match data. They investigate causes and consequences of variability, contribute to determine causality, suggest hypotheses and tests, determine the separate effect of a parameter, and tend to provide coherent explanations.

Most models of tissue mechanics hypothesize material properties and distribution of forces, which are often not measured. Not only quantitative measurements will allow us restrict the number of unknown parameters but also help us making the right hypotheses, by testing falsifiable predictions of different models. Models could then confront images (or movies) and force measurements to determine the tissue material properties. This step is essential to develop predictive models of tissue mechanics, in an attempt to explain how cells-level changes (deformation, growth, displacement, neighbour swapping, divisions and apoptoses) do determine, though mechanical interactions, the final shape and size of a tissue (Tlili et al., 2015).

Acknowledgments
The content of this article is the work of the participants to the informal and intense "Forces in tissues" workshop held in Paris 7 University, May 2014. The text has been written by Kaoru Sugimura, François Graner, Pierre-François Lenne, organisers of the workshop. For details and participants list, see http://www.msc.univ-paris-diderot.fr/tissue-stress.

References:

Anderson, A. R. A., Chaplain, M. A. J. and Rejniak, K. A. (eds) (2007). Single cell based models in biology and medicine. Basel: Birkhäuser.

Bambardekar, K., Clément, R., Blanc, O., Chardès, C. and Lenne, P.-F. (2015). Direct laser manipulation reveals the mechanics of cell contacts *in vivo*. *Proc. Natl. Acad. Sci. USA* **112**, 1416-21.

Beauzamy, L., Nakayama, N. and Boudaoud, A. (2014). Flowers under pressure: ins and outs of turgor regulation in development. *Ann. Bot.* **114**, 1517-33.

Behrndt, M., Salbreux, G., Campinho, P., Hauschild, R., Oswald, F., Roensch, J., Grill, S. W. and Heisenberg, C. P. (2012). Forces driving epithelial spreading in *zebrafish* gastrulation. *Science* **338**, 257-60.

Bonnet, I., Marcq, P., Bosveld, F., Fetler, L., Bellaiche, Y. and Graner, F. (2012). Mechanical state, material properties and continuous description of an epithelial tissue. *J. R. Soc. Interface* **9**, 2614-23.

Borghi, N., Sorokina, M., Shcherbakova, O. G., Weis, W. I., Pruitt, B. L., Nelson, W. J. and Dunn, A. R. (2012). E-cadherin is under constitutive actomyosin-generated tension that is increased at cell-cell contacts upon externally applied stretch. *Proc. Natl. Acad. Sci. USA* **109**, 12568-73.

Brodland, G.W. (2004). Computer modeling of cell sorting, tissue engulfment and related phenomena: a review, *ASME Appl. Mech. Rev.* **57**, 1-30.

Brodland, G. W., Conte, V., Cranston, P. G., Veldhuis, J., Narasimhan, S., Hutson, M. S., Jacinto, A., Ulrich, F., Baum, B. and Miodownik, M. (2010). Video force microscopy reveals the mechanics of ventral furrow invagination in Drosophila. *Proc. Natl. Acad. Sci. USA* **107**, 22111-6.

Brodland, G. W., Veldhuis, J. H., Kim, S., Perrone, M., Mashburn, D. and Hutson, M. S. (2014). CellFIT: a cellular force-inference toolkit using curvilinear cell boundaries. *PLoS One* **9**, e99116.

Brunet, T., Bouclet, A., Ahmadi, P., Mitrossilis, D., Driquez, B., Brunet, A. C., Henry, L., Serman, F., Bealle, G., Menager, C. et al. (2013). Evolutionary conservation of early mesoderm specification by mechanotransduction in Bilateria. *Nat. Commun.* 4, 2821.

Cai, D., Chen, S. C., Prasad, M., He, L., Wang, X., Choesmel-Cadamuro, V., Sawyer, J. K., Danuser, G. and Montell, D. J. (2014). Mechanical feedback through E-cadherin promotes direction sensing during collective cell migration. *Cell* **157**, 1146-59.

Campàs, O., Mammoto, T., Hasso, S., Sperling, R. A., O'Connell, D., Bischof, A. G., Maas, R., Weitz, D. A., Mahadevan, L. and Ingber, D. E. (2014). Quantifying cell-generated mechanical forces within living embryonic tissues. *Nat. Methods* **11**, 183-9.

Chiou, K. K., Hufnagel, L. and Shraiman, B. I. (2012). Mechanical stress inference for two dimensional cell arrays. *PLoS Comput. Biol.* **8**, e1002512.

Curtis, A., Sokolikova-Csaderova, L. and Aitchison, G. (2007). Measuring cell forces by a photoelastic method. *Biophys. J.* **92**, 2255-2261.

Davidson, L. and Keller, R. (2007). Measuring mechanical properties of embryos and embryonic tissues. *Methods Cell Biol.* **83**, 425–439.

Desprat, N., Supatto, W., Pouille, P. A., Beaurepaire, E. and Farge, E. (2008). Tissue deformation modulates twist expression to determine anterior midgut differentiation in Drosophila embryos. *Dev. Cell* **15**, 470–477.

Evans, E. and Yeung, A. (1989). Apparent viscosity and cortical tension of blood granulocytes determined by micropipet aspiration. *Biophys. J* **56**, 151–160.

Farhadifar, R., Röper, J. C., Aigouy, B., Eaton, S. and Jülicher, F. (2007). The influence of cell mechanics, cell-cell interactions, and proliferation on epithelial packing. *Curr. Biol.* **17**, 2095–2104.

Forouzesh, E., Goel, A., Mackenzie, S. A. and Turner J. A. (2013). In vivo extraction of Arabidopsis cell turgor

pressure using nanoindentation in conjunction with finite element modeling. *Plant J.* **73**, 509-20.

Foty, R., Forgacs, G., Pfleger, C. and Steinberg, M. (1994). Liquid properties of embryonic tissues: Measurement of interfacial tensions. *Phys. Rev. Lett.* **72**, 2298–2301.

Fung, Y. C. (1993). Biomechanics: Mechanical properties of living tissues. Berlin: Springer.

Gomez-Martinez, R., Hernandez-Pinto, A. M., Duch, M., Vazquez, P., Zinoviev, K., de la Rosa, E. J., Esteve, J., Suarez, T. and Plaza, J. A. Silicon chips detect intracellular pressure changes in living cells. *Nat. Nanotechnol.* 8, 517-21.

Grashoff, C., Hoffman, B. D., Brenner, M. D., Zhou, R., Parsons, M., Yang, M. T., McLean, M. A., Sligar, S. G., Chen, C. S., Ha, T. et al. (2010). Measuring mechanical tension across vinculin reveals regulation of focal adhesion dynamics. *Nature* **466**, 263-6.

Guevorkian, K., Colbert, M.-J., Durth, M., Dufour, S. and Brochard-Wyart, F. (2010). Aspiration of biological viscoelastic drops. *Phys. Rev. Lett.* **104**, 218101.

Heisenberg, C. P. and Bellaïche, Y. (2013). Forces in tissue morphogenesis and patterning. *Cell* **153**, 948-62.

Hutson, M. S., Tokutake, Y., Chang, M.-S., Bloor, J. W., Venakides, S., Kiehart, D. P. and Edwards, G. S. (2003). Forces for morphogenesis investigated with laser microsurgery and quantitative modeling. *Science* **300**, 145–149.

Ishihara, S. and Sugimura, K. (2012). Bayesian inference of force dynamics during morphogenesis. *J. theor. Biol.* **313**, 201-11.

Ishihara, S., Sugimura, K., Cox, S. J., Bonnet, I., Bellaiche, Y. and Graner, F. (2013). Comparative study of non-invasive force and stress inference methods in tissue. *Eur. Phys. J. E* **36**, 9859.

Keller, E. F. (2002). Making sense of life: explaining biological development with models, metaphors, and machines. Harvard: Harvard University Press.

Kiehart, D. P., Galbraith, C. G., Edwards, K. A., Rickoll, W. L., Montague, R. A. (2000) Multiple forces contribute to cell sheet morphogenesis for dorsal closure in Drosophila. *J. Cell Biol.* **149**, 471–490.

Kolb E., Hartmann C., and Genet P. (2012). Radial force development during root growth measured by photoelasticity. *Plant and Soil* **360**, 19-35.

Krieg, M., Arboleda-Estudillo, Y., Puech, P.-H., Käfer, J., Graner, F., Müller, D. J. and Heisenberg, C.-P. (2008). Tensile forces govern germ-layer organization in zebrafish. *Nat. Cell Biol.* **10**, 429–436.

Krieg, M., Dunn, A. R. and Goodman, M. B. (2014). Mechanical control of the sense of touch by beta-spectrin. *Nat. Cell Biol.* **16**, 224-33.

Labouesse, M. (éd). (2011). Forces and tension in development, *Curr. Top. Dev. Biol.* **95**, 2-270.

Landsberg, K. P., Farhadifar, R., Ranft, J., Umetsu, D., Widmann, T. J., Bittig, T., Said, A., Jülicher, F. and Dahmann, C. (2009). Increased Cell Bond Tension Governs Cell Sorting at the Drosophila Anteroposterior Compartment Boundary. *Curr. Biol.* **19**, 1950-1955.

Lecuit, T., Lenne, P. F. and Munro, E. (2011). Force generation, transmission, and integration during cell and tissue morphogenesis. *Annu. Rev. Cell Dev. Biol.* **27**, 157-84.

Lomakina, E. B., Spillmann, C. M., King, M. R. and Waugh, R. E. (2004). Rheological analysis and measurement of neutrophil indentation. *Bioph. J* **87**, 4246–4258.

Maître, J.-L., Berthoumieux, H., Krens, S. F. G., Salbreux, G., Jülicher, F., Paluch, E. and Heisenberg, C.-P. (2012). Adhesion functions in cell sorting by mechanically coupling the cortices of adhering cells. *Science* **338**, 253-256

Mammoto, A., Mammoto, T. and Ingber, D. E. (2012). Mechanosensitive mechanisms in transcriptional regulation. *J. Cell Sci.* 125, 3061-73.

Marmottant, P., Mgharbel, A., Käfer, J., Audren, B., Rieu, J.-P., Vial, J.-C., van der Sanden, B., Marée, A. F. M., Graner, F. and Delanoë-Ayari, H. (2009). The role of fluctuations and stress on the effective viscosity of cell aggregates. *Proc. Natl. Acad. Sci. USA* **106**, 17271–17275.

Mayer, M., Depken, M., Bois, J. S., Jülicher, F. and Grill, S. W. (2010). Anisotropies in cortical tension reveal the physical basis of polarizing cortical flows. *Nature* **467**, 617–621.

Meng, F., Suchyna, T. M. and Sachs, F. (2008). A fluorescence energy transfer-based mechanical stress sensor for specific proteins in situ. *FEBS J* **275**, 3072-87.

Miyawaki, A. (2011). Development of probes for cellular functions using fluorescent proteins and fluorescence resonance energy transfer. *Annu. Rev. Biochem.* **80**, 357-73.

Nienhaus, U., Aegerter-Wilmsen, T. and Aegerter, C. M. (2009). Determination of mechanical stress distribution in Drosophila wing discs using photoelasticity. *Mech. Dev.* **126**, 942-9.

Oates, A. C, Gorfinkiel, N., González-Gaitán, M., and Heisenberg, C.-P. (2009). Quantitative approaches in developmental biology. *Nat. Gen.* **10**, 517-530.

Oddershede, L. B. (2012). Force probing of individual molecules inside the living cell is now a reality. *Nat. Chem. Biol.* **8**, 879-86.

Oldenbourg, R. (2005) Polarization microscopy with the LC-PolScope. In *Live cell imaging: A laboratory manual.* (ed. R. D. Goldman and D. L. Spector), pp. 205-237. Cold Spring Harbor, NY: Cold Spring Harbor Laboratory Press.

Paluch, E. K. (ed.), (2015). Biophysical methods in cell biology. *Meth. Cell Biol.* **125**, 1-488.

Paluch, E. and Heisenberg, C.-P. (2009). Biology and physics of cell shape changes in development. *Current biology* **19**, R790–9.

Rauzi, M., Verant, P., Lecuit, T. and Lenne, P.-F. (2008). Nature and anisotropy of cortical forces orienting Drosophila tissue morphogenesis. *Nat. Cell Biol.* **10**, 1401–1410.

Sampathkumar, A., Yan, A., Krupinski, P. and Meyerowitz, E. M. (2014). Physical forces regulate plant development and morphogenesis. *Curr. Biol.* **24**, R475-83.

Savin, T., Kurpios, N. A., Shyer, A. E., Florescu, P., Liang, H., Mahadevan, L. and Tabin, C. J. (2011). On the growth and form of the gut. *Nature* **476**, 57-62.

Schluck, T. and Aegerter, C. M. (2010). Photo-elastic properties of the wing imaginal disc of Drosophila. *Eur. Phys. J. E* **33**, 111-115.

Shribak, M. and Oldenbourg, R. (2003). Techniques for fast and sensitive measurements of two-dimensional birefringence distributions. *Appl. Opt.* **42**, 3009-3017.

Sugimura, K. and Ishihara, S. (2013). The mechanical anisotropy in a tissue promotes ordering in hexagonal cell packing. *Development* **140**, 4091-101.

Tanase, M., Biais, N. and Sheetz, M. (2007). Magnetic tweezers in cell biology. *Methods Cell Biol.* **83**, 473–493.

Tlili, S., Gay, C., Graner, F., Marcq, P., Molino, F. and Saramito, P. (2015). Mechanical formalism for tissue dynamics. Eur. Phys. J. E, in press.

Trejo, M., Douarche, C., Bailleux, V., Poulard, C., Mariot, S., Regeard, C. and Raspaud, E. (2013). Elasticity and wrinkled morphology of Bacillus Subtilis pellicles. *Proc. Natl. Acad. Sci. USA*, **110**, 2011-16.

Vogel, A. and Venugopalan, V. (2003). Mechanisms of Pulsed Laser Ablation of Biological Tissues. *Chem. Rev.* **103**, 577–644.

Watanabe, T. M., Imada, K., Yoshizawa, K., Nishiyama, M., Kato, C., Abe, F., Morikawa, T. J., Kinoshita, M., Fujita, H. and Yanagida, T. Glycine insertion makes yellow fluorescent protein sensitive to hydrostatic pressure. *PLoS One* **8**, e73212.

Zhou, J., Pal, S., Maiti, S. and Davidson, L. A. (2015). Force production and mechanical accommodation during convergent extension. *Development* **142**, 692-701.

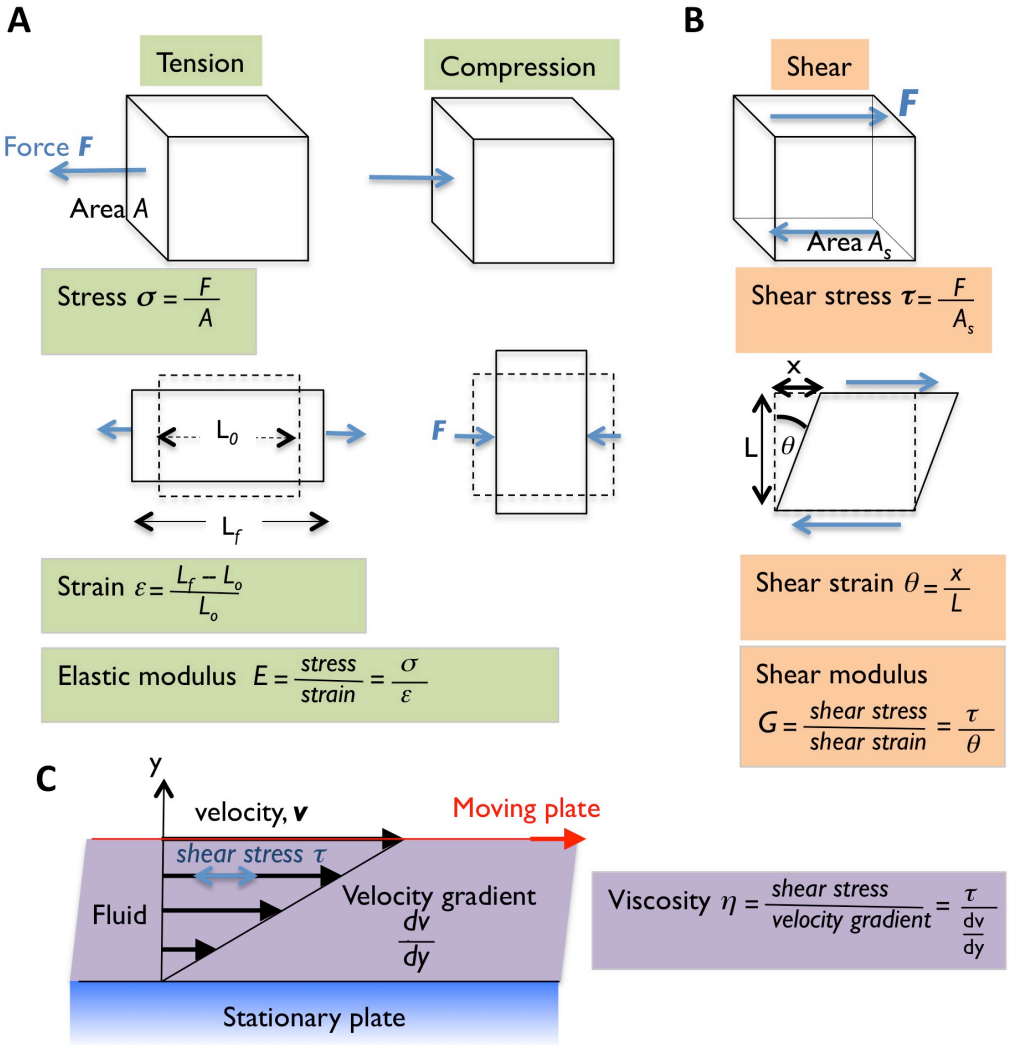

Figure 1:
Definition of mechanical terms.
(A) Uniaxial compression. When a material experiences a force perpendicular to one of its surfaces, stress is defined as the ratio of the force to the surface area A. Force has a magnitude and a direction; tension and compression correspond to forces pointing respectively outwards and inwards of the body. Stress is a force per unit area, which units is Pascals. Strain is defined as the relative increment in length. The elastic modulus is the ratio of stress to strain, also known as the Young modulus, which unit is also in Pascals.
(B) Shear. When a material experiences a force parallel to one of its surfaces, the deformation is called shear. Shear strain is defined by an angle. Shear modulus is defined as the ratio of shear stress to shear strain.
(C) Velocity gradient in a fluid. When a fluid experiences a shear stress, it flows but resists deformation. In a laminar flow between two plates, one moving and the other being stationary, the shear stress is proportionnal to the velocity gradient. The viscosity is defined as the ratio of the shear stress to velocity gradient, which is homogeneous in a simple fluid.

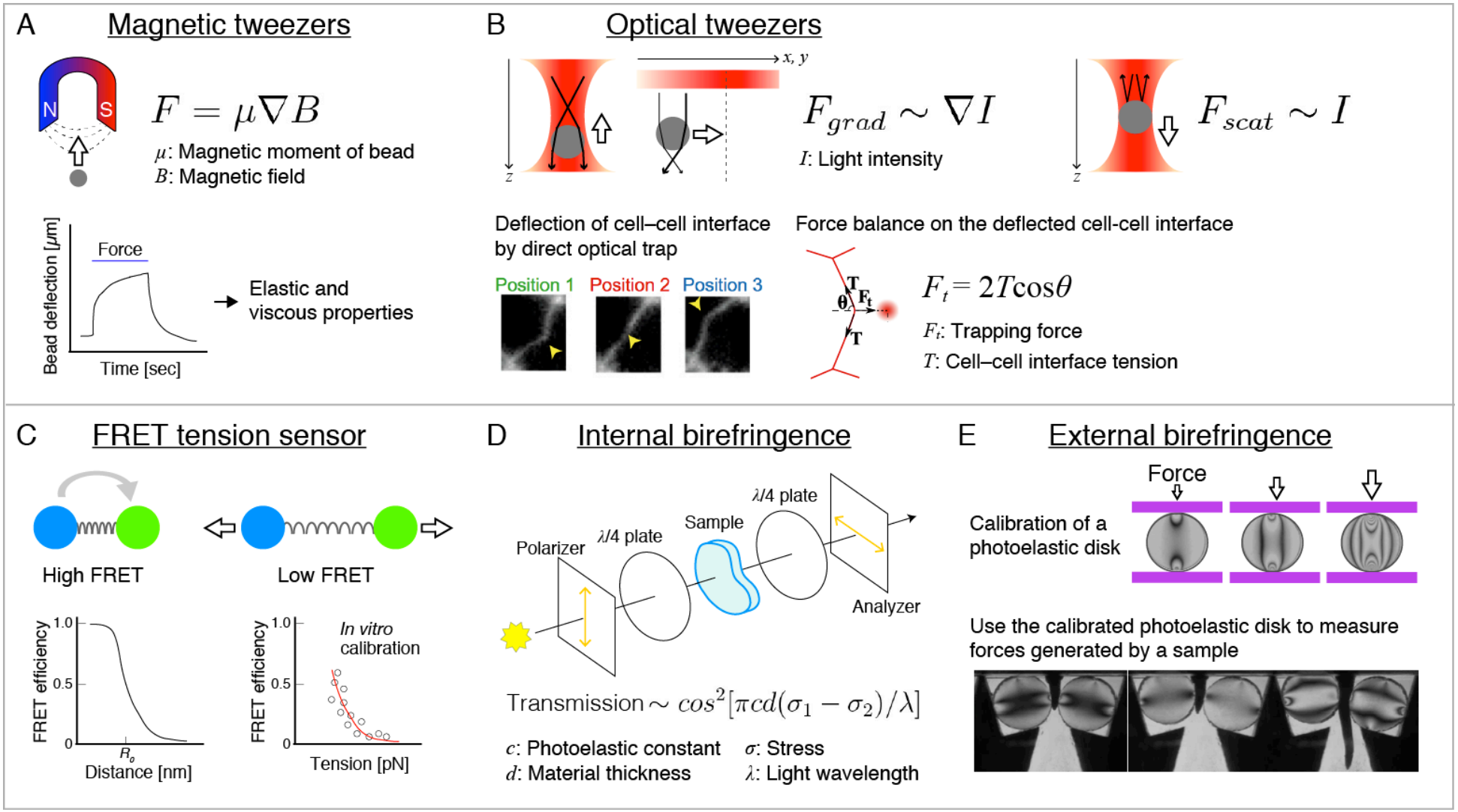

Figure 2:
Illustration of each method: see text for details.
(A) Magnetic tweezers. (B) Optical tweezers. (C) FRET tension sensor. (C) Internal birefringence. (E) External birefringence.

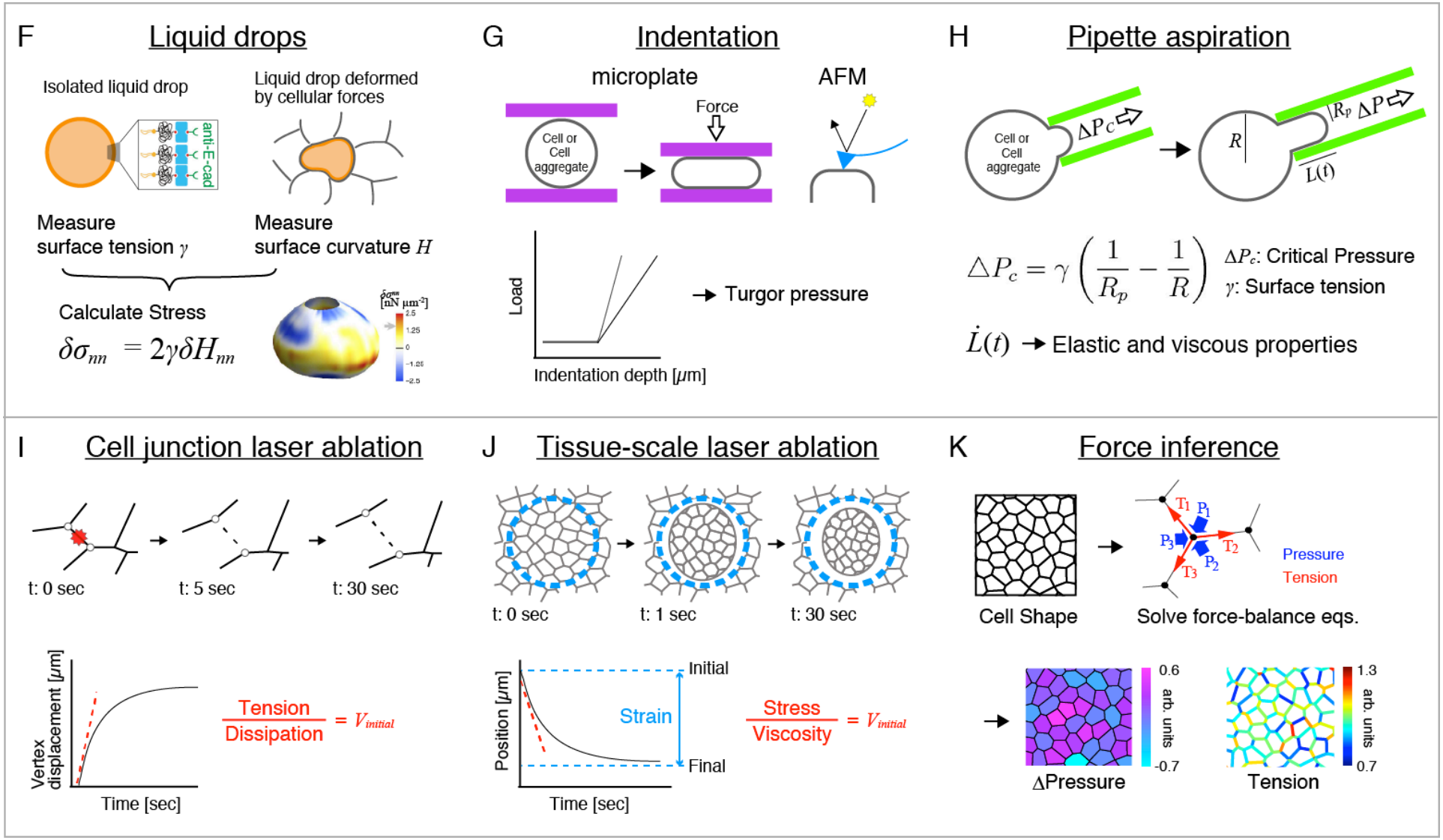

Figure 2, continued:
(F) Liquid drop stress sensor. (G) Indentation. (H) Pipette aspiration. (I) Subcellular laser ablation. (J) Tissue scale laser ablation. (K) Force inference.
Adapted with permission from: (B) Bambardekar et al., 2015, (C) Grashoff et al., 2011, (E) Kolb et al., 2012, (F) Campàs et al., 2014, (H) Guevorkian et al., 2010, (J) Bonnet et al., 2012, (K) Ishihara and Sugimura, 2012.

	Measured quantities	Measurable range	Time scale *	Size scale **	Advantages
Optical/ magnetic tweezers	Cell junction tension	pN-nN	ms-min	0.1 μm – 10 μm	Non-contact Absolute measurements
FRET force probe	Intramolecular tension	pN	>s	nm	Molecular measurements
Birefringence	Tissue-scale stress	>10kPa	>s	>μm	Global
Liquid drops	Cell-scale stress	4- 30 mN/m 0.3-60 kPa	0.1 s-hours	>5μm	Absolute measurements Parallel
Indentation/ microplates	Cell wall tension, aggegate surface tension	0.1 Pa	s-hours	Few μm - 100 μm	Absolute measurements
Pipette aspiration	Pressure, stress	μN/m -10s mN/m	>10s	Few μm - 100 μm	Absolute measurements
Subcellular laser ablation	Cell junction tension to dissipation ratio	NA	s-min	0.1 μm - 10 μm	Non-contact
Tissue-scale laser ablation	Tissue stress to viscosity ratio	NA	s-min	100 μm - mm	Non-contact
Force inference	Relative cell junction tension, cell pressure	NA	NA	>μm	Image based – Global

* Time scale of the mechanical processes that can be probed
** Size scale of the mechanical processes or mechanical elements that can be probed

Table 1:
Synthetic view of method comparisons.